Supporting Information

Mechanically Robust, Highly Sensitive, Resilient, and Degradable Dual Physically Cross-Linked Hydrogel for Heart Rate Health Detection

Xiang Di[a]，Liqi Li[a], Jinjiang Dai[a], Shiyuan Fan[a], Jiawen Hou[b], Guolin Wu[b]，Xuefeng Gao[c], Yuan Li[a], Chungang Yuan[a,*]

[a]Hebei Key Laboratory of New Energy Environmental Safety and Resource Utilization, Department of Environmental Science and Engineering, North China Electric Power University, Baoding E-mail: cgyuan@ncepu.edu.cn; Fax: +86-312-7525509

[b]Key Laboratory of Functional Polymer Materials Institute of Polymer Chemistry College of Chemistry Nankai University Tianjin 300071, P. R. China

[c]National Pesticide Engineering Research Center (Tianjin), College of Chemistry, Nankai University, 300071, Tianjin, China

Experimental Section/Methods

Materials

Hexadecyl methacrylate (HMA), cetyltrimethylammonium bromide (CTAB), acrylamide (AM), and persulfate (KPS) were supplied by Aladdin Reagent Company (Shanghai. China). Phytic acid (PA) was obtained from TCI (Shanghai. China). Lithium chloride (LiCl, 99.5%) was purchased from Energy Chemical. Deionized water was used for all experiments.

Fabrication of physically cross-linked hydrogels

Physical hydrogels were fabricated by a two-step procedure via free-radical polymerization method. Firstly, the appropriate amounts of CTAB and LiCl were dissolved in deionized water to obtain a mixed solution, HMA was added and stirred thoroughly to ensure complete dissolution. Then, AM and PA monomers were added sequentially and stirring was continued until complete dissolution. KPS was added as initiator with continuous stirring. The mixed solution was degassed under nitrogen for 10 min, quickly poured into glass molds and kept at 60°C for 3 h to yield the obtained hydrogel. The proportion of HMA and PA employed in the preparation process can be adjusted in order to yield samples with a range of distinct properties. The compositions of all the samples with different monomers are presented in Table S1.

Characterization

Fourier transform infrared (FTIR) spectroscopy (A225/Q Platinum ATR) was employed

to elucidate the structural characteristics of diverse hydrogel materials. X-ray diffraction (XRD) tests were conducted to ascertain the degree of crystallinity of the materials utilizing an X-ray diffractometer (Rigaku Smart Lab, Japan) with 2θ = 10°~60°. The morphology of the lyophilized samples was observed using a scanning electron microscope (SEM, TM4000Plus II, Japan). Low-field NMR spectroscopy was conducted using a low-field spectrometer (Bruker Minispec MQ20) with a proton resonance frequency of 20 MHz.

Mechanical measurements

Tensile testing of the hydrogels was conducted at room temperature using a universal testing machine (UTM6103, Suns Technology Stock Co., Ltd., China). The hydrogel samples were cut into rectangular specimens with dimensions of 50 mm×5 mm×1 mm. The uniaxial tensile rate was 50 mm/min, while the cyclic loading-unloading test rate was 100 mm/min. The samples employed in the compression tests were cylindrical with a diameter of 12 mm and a height of 13 mm, and the compression rate was maintained at 5 mm/min. The Young's modulus was determined by calculating the slope of the stress-strain curves between the 5-20% strain ratios. Toughness was calculated by measuring the area under the stress-strain curve. To ensure accuracy and reliability, each tensile test was performed at least three times, and the average of the data was calculated.

Rheological Measurements

A series of linear oscillatory shear and strain scanning tests were conducted using a dynamic rheometer (DHR-2, TA Instruments) with parallel plates of 25 mm diameter. To prevent the gel surface from drying, a layer of liquid paraffin was applied to the outer edges. Strain amplitude scans were carried out in the range of 0.1% to 2000% at a fixed frequency of 1 Hz, with the objective of determining the linear viscoelastic range. Dynamic frequency scans were performed in the linear region at a constant strain of 0.5%. The study analyses the microscopic self-healing properties through the means of alternating step-strain scanning measurements (0.5% and 1000%) utilising 1 Hz oscillatory forces, which were employed for the purpose of characterizing the disruption and reorganization of the internal network.

Thermodynamic measurements

The phase transition temperature of the hydrogels was determined by differential scanning calorimetry (DSC) at a rate of 5 °C min^{-1}. The temperature range of the test was 25°C to -55°C under nitrogen atmosphere. Each 40 μl aluminium disc contained approximately 10 mg of sample. To ensure accuracy, each sample was tested three times and the data were normalized to the final experimental results.

Conductivity measurements

An electrochemical workstation (Shanghai Chenhua CHI-660E) was employed to investigate the conductivity and relative resistance of the hydrogel sensor in different states. The conductivity was calculated by the following formula:

$$\sigma = \left(\frac{L}{AR}\right)$$

where L is the thickness between the two metal electrodes, A is the area of the measured contact surface of the gel sample, and R is the measured resistance of the hydrogel.

The relative resistance $\Delta R/R_0$ was calculated according to the following formula:

$$\frac{\Delta R}{R_0} = \left(\frac{R - R_0}{R_0}\right) * 100\%$$

where R_0 and R are the resistance of original hydrogel sensor and the same sample under strain, respectively.

The GF was defined as follows:

$$GF = \frac{\Delta R/R_0}{\varepsilon}$$

where $\Delta R/R_0$ is the change in relative resistance of the strain sensor and ε is the corresponding change in strain of the sample.

Low-field ^{1}H NMR spectroscopy

Low-field NMR spectroscopy was conducted using a low-field spectrometer (Bruker Minispec MQ20) with a proton resonance frequency of 20 MHz. The typical p/2 pulse length of the Minispec was ~3 μs and the dead time of the receiver was ~13 μs. Magic-sandwich echo (MSE) pulse sequence was applied to reunite the lost signal. In multiphase materials, rigid components with a strong proton dipole coupling possess fast proton signal decay, while the mobile component exhibits a slow free-induction decay (FID) signal due to the averaging effect. Therefore, the regained MSE-FID signal can be fitted to the following equation:

$$I(t) = f_{r*}exp(-(t/T_{2r})^2) + f_{i*}exp(-(t/T_{2i})^{ni}) + f_{s*}exp(-(t/T_{2s})^{ns})$$

where fr, fi, and fs represent the relative contents of the rigid component, intermediate component, and soft component, respectively, and $f_r+f_i+f_s = 1$. T_{2r}, T_{2i}, and T_{2s} indicate the relaxation time of the rigid component, intermediate component, and mobile component, respectively ($T_{2r} < T_{2i} < T_{2s}$).

Proton MQ NMR experiments

NMR spectroscopy is a convenient and accurate technique to obtain information about the dynamics of polymer networks and solid structures. In general, two sets of data, the double quantum (DQ) and the reference signal intensity (I_{DQ} and I_{ref}), can be obtained from

MQ NMR experiments. The sum of these two signals is the MQ intensity, which is affected by chain segment fluctuations. Therefore, it needs to be normalized in order to obtain the normalized DQ intensity as follows:

$$I_{nDQ}(\tau_{DQ}, D_{res}) = 0.5(1-\exp\{-(0.378 D_{res}\tau_{DQ})^{1.5}\} * \cos[0.583 D_{res}\tau_{DQ}]$$

$$P(D_{res}) = \frac{1}{\sqrt{2\pi}\sigma D_{res}} e^{-(\ln\left(\frac{D_{res}}{D_m}\right))^2/2\sigma^2}$$

Such a normalization process eliminates the temperature-dependent chain segment kinetic effects so that the normalized DQ intensity accumulation is completely dependent on the network and the D_{res} is determined by the confined structure.

Weight Swelling Rate Measurements

The classical weighing method was utilized to determine the swelling rate of hydrogels. The methodology is as follows: initially, the prepared hydrogel was weighed to record the initial weight (W_p), then placed in deionized water to fully dissolve, and weighed at intervals to record the weight (W_r) until the gel quality no longer changed and reached dissolution equilibrium.

The swelling ratio was calculated according to the following formula:

$$Swell\ ratio(\%) = \left(\frac{w_r - w_p}{w_p}\right) \times 100\%$$

At least 3 samples of each type are tested and the average value is taken as the final swelling ratio of the gel.

Hydrogel adhesion test

The adhesion properties of the hydrogel were tested by a universal testing machine (UTM6103, Suns Technology Stock Co., Ltd., China) at room temperature in a lap-shear test. The hydrogel was adhered to the center of two pieces of material in a sandwich structure with an adhesion area of 20 mm×20 mm, and the test was carried out at a tensile rate of 50 mm/min. The adhesion strength was determined as the maximum load divided by the adhesion area (Fmax/S).

Bioelectric Signal Monitoring

Electrocardiographic (ECG) signals were obtained from hydrogel and commercial electrodes. The hydrogel electrodes were cut into round pieces using a hole punch, ensuring that they were of the same size as the gel in the original ECG electrode sheets. The conductive hydrogel was then used to place inside the red, yellow and green electrodes of the detector

(Heal Force PC-80B ECG). The ECG signal was then acquired using the ECG detector. The ECG electrode patches, prepared based on the conductive hydrogel, were adhered to the left chest, right chest and right abdomen of the tester using the three-conductor method. The tester was kept sitting still to initiate the ECG signal test. The PC-80B ECG detector was then connected to the ECG Viewer Manager signal collection software to obtain ECG signal images.

Ethical statement

All experiments involving human subjects have been followed the guidelines of The Code of Ethics of the World Medical Association. All the volunteers employed in the adhesion test and the human motion sensing test are informed of this manuscript, and the gender of the volunteers had no impact on the research results. The informed consent has been obtained for experimentation with human subjects.

Degradability measurements

The in vitro degradation behavior of hydrogels was assessed by measuring the mass reduction of the hydrogels. The prepared hydrogels were freeze-dried and weighed (W_0) using a freeze-dryer. The hydrogels were prepared as previously described and the medium was supplemented with PBS every two days. Physical images of the hydrogels were taken at regular intervals during the degradation process. The water on the surface of the hydrogel was immediately drained by filtration. The weight of the paper (W_t) was measured using an analytical balance, and the degradation rate was calculated as (W_0- W_t)/ W_0 × 100%, while the residual rate was 1-(W_0- W_t)/ W_0 × 100%.

Cytotoxicity test

The CCK-8 method was used to characterize the cytocompatibility of the gel extracts[1-3]. First, the gel was soaked in 75% ethanol for 2 h to sterilize and washed three times with PBS adequately, and then the gel was soaked in DMEM medium for 24 h at 37 ℃ to obtain the gel extract. NIH3T3 fibroblasts with a density of $8x10^3$ cells/well were inoculated in a 96-well plate, then added to DMEM medium and cultured in a cell culture incubator containing 5% CO_2 for 24h to obtain a monolayer of evenly distributed cells. The gel extracts (100μg/ml, 500μg/ml) were passed through a 0.22 μm sterile filter to remove biological contaminants, and then 100 μl of DMEM was replaced by 100 μl of extract, and the wells without replacement were used as controls. After 24 h of incubation, Finally, cell viability was tested using the CCK-8 cell viability assay and normalized to the control group.

Table S1. Recipes for hydrogels

Hydrogels	HMA (mg)	PA (mg)	AM (g)	CTAB (g)	KPS (mg)	Water (mL)	LiCl (g)
P(H_{25}-AM)/PA_0	**25**	**0**	**2**	**0.4**	**20**	**5**	**0.2**
P(H_{50}-AM)/PA_0	**50**	**0**	**2**	**0.4**	**20**	**5**	**0.2**
P(H_{75}-AM)/PA_0	**75**	**0**	**2**	**0.4**	**20**	**5**	**0.2**
P(H_{100}-AM)/PA_0	**100**	**0**	**2**	**0.4**	**20**	**5**	**0.2**
P(H_{125}-AM)/PA_0	**125**	**0**	**2**	**0.4**	**20**	**5**	**0.2**
P(H_{75}-AM)/$PA_{0.1}$	**75**	**0.1**	**2**	**0.4**	**20**	**5**	**0.2**
P(H_{75}-AM)/$PA_{0.2}$	**75**	**0.2**	**2**	**0.4**	**20**	**5**	**0.2**
P(H_{75}-AM)/$PA_{0.4}$	**75**	**0.4**	**2**	**0.4**	**20**	**5**	**0.2**
P(H_{75}-AM)/$PA_{0.8}$	**75**	**0.8**	**2**	**0.4**	**20**	**5**	**0.2**

Table S2. Summary of recently reported physical crosslinking conducttive hydrogels

Sample	Stress (kPa)	Strain (%)	GF	Freezing Resistance (℃)	Ionic Conductivity (S/m)	Source
$P(H_{75}\text{-AM})/PA_{0.1}$	437	988	1.16	-36.7	1.7	This study
PAAm-PA-CNC	300	670	\	-27.1	0.112	Ref.1[4]
WL-0 G5	120	567	0.58	-29	0.59	Ref.2[5]
PAA/Phyx	144.7	870	0.27	-20	\	Ref.3[6]
PEG-HEMA	49.9	529.7	1.076	-20	0.55	Ref.4[7]
PA-LMP/PVA	460	676.9	1	\	2.25	Ref.5[8]
Cu^{2+}/PVA/AM	226	1168	0.124	\	3×10^{-5}	Ref.6[9]
PB-PACS-PM_3	36	800	1.2	\	1.5	Ref.7[10]
DN-4-Y	367	800	0.928	\	0.076	Ref.8[11]
PAM/SA/TA-CNTs	108.3	727	1.2	-23	0.266	Ref.9[12]
TA@Fe-Cel-PA	250	500	0.75	\	1	Ref.10[13]

Table S3. Hydrogel double quantum average residual dipole coupling constant

Sample	Dm/2π (kHz)	σ
$P(H_{75}\text{-AM})/PA_0$	1.70	0.42

$P(H_{75}\text{-AM})/PA_{0.1}$	**1.73**	**0.56**

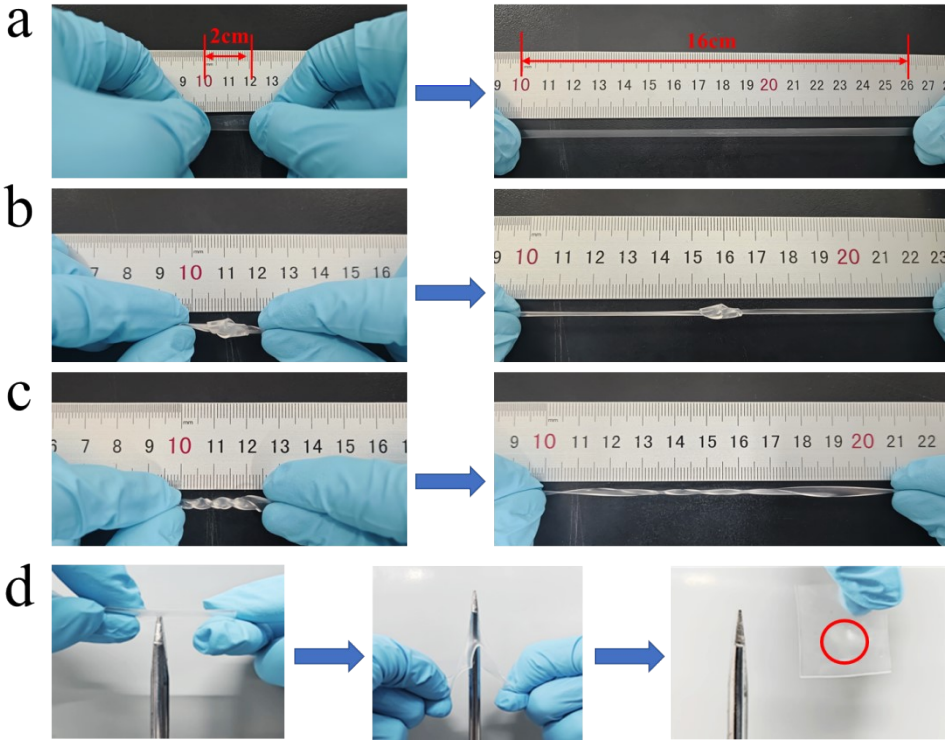

Figure S1. (a-d) $P(H_{75}\text{-AM})/PA_{0.1}$ hydrogel was subjected to stretching, knotting, twisting and puncture tests.

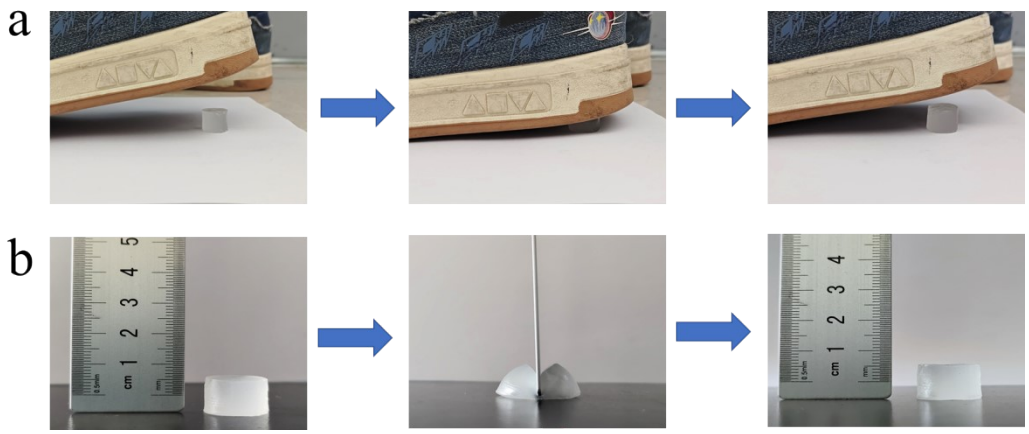

Figure S2. (a-b) Compression resistance of $P(H_{75}\text{-AM})/PA_{0.1}$ hydrogel in different scenarios.

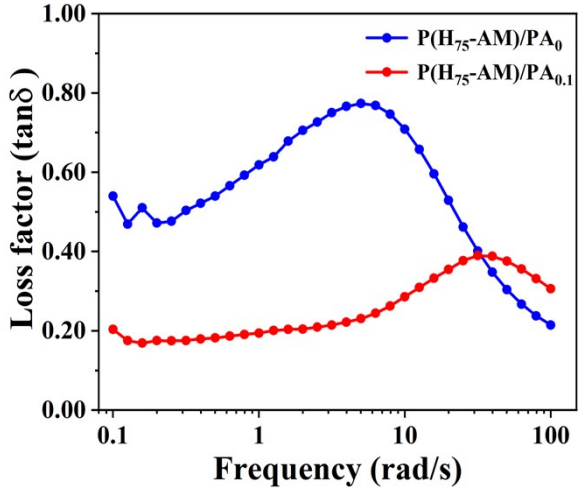

Figure S3. The loss factor (tanδ) of hydrogel at different frequency.

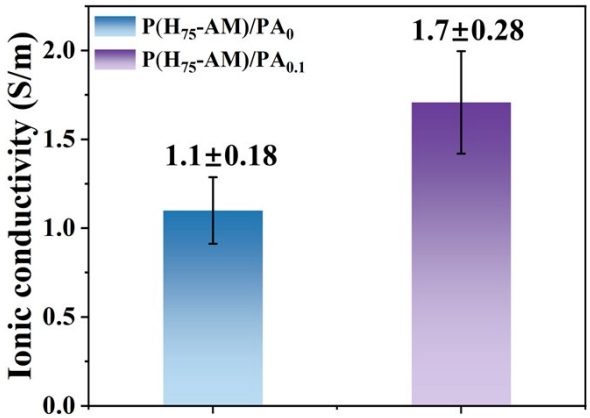

Figure S4. The ionic conductivity of different hydrogels.

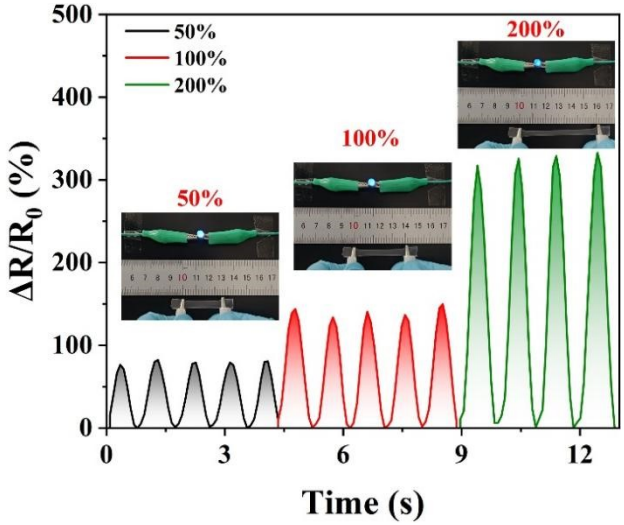

Figure S5. (a-d) Variation of LED light brightness under different tensile strains for P(H_{75}-AM)/$PA_{0.1}$.

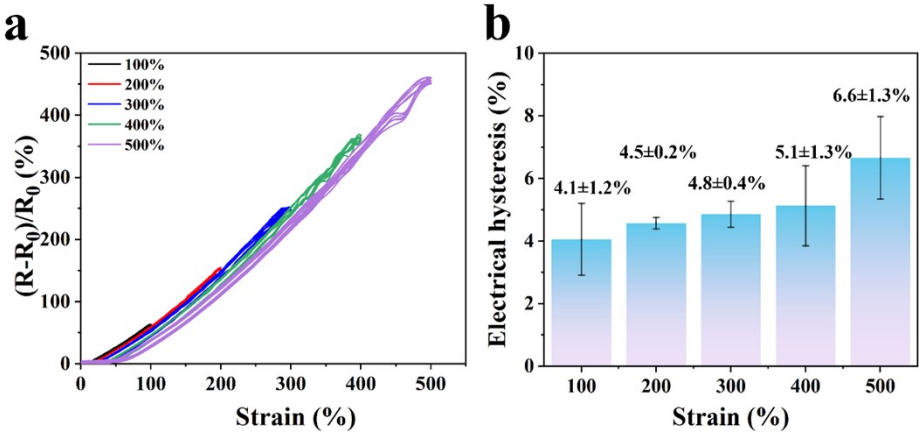

Figure S6. (a) The relative resistance curves and (b) electrical hysteresis under loading-unloading cycles over a wide strain range (100-500%).

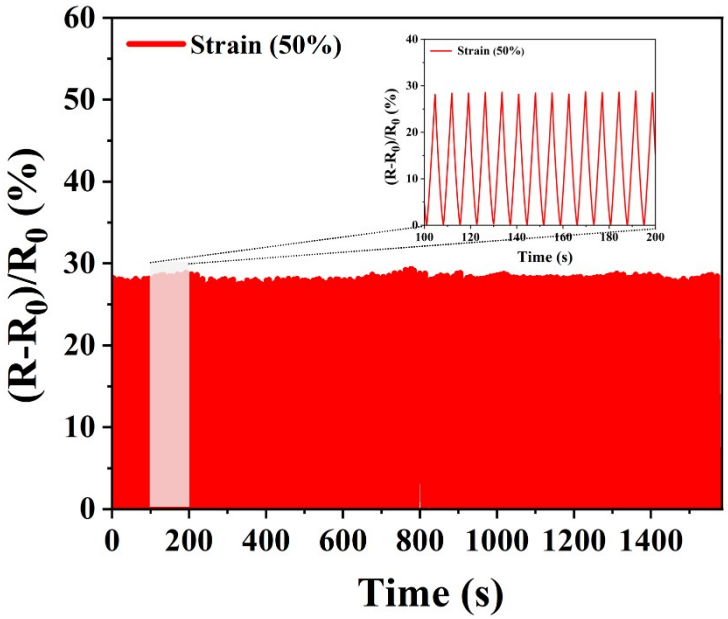

Figure S7. Stability of the sensor relative to the resistance signal at 50% strain for 200 cycles after 10 days of placement.

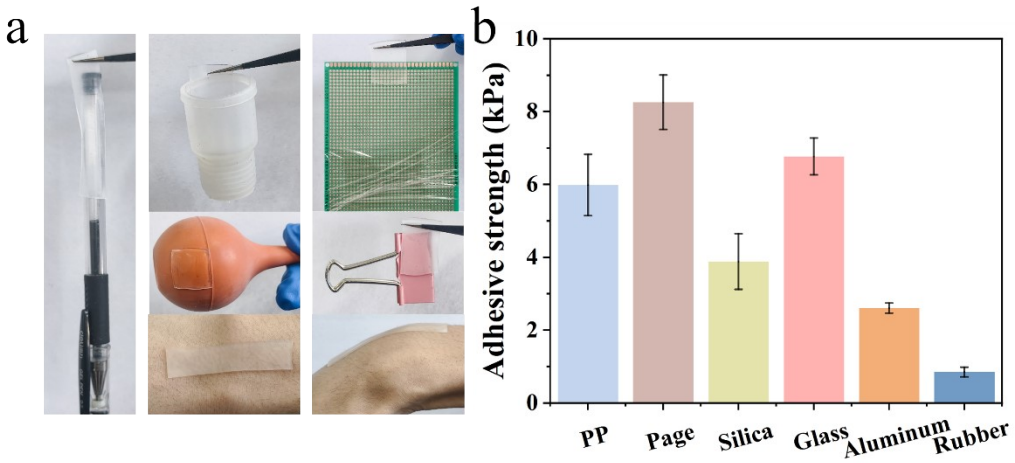

.

Figure S8. (a) Demonstration of P(H_{75}-AM)/$PA_{0.1}$ hydrogel adhesion to different materials and (b) Strength of P(H_{75}-AM)/$PA_{0.1}$ hydrogel adhesion

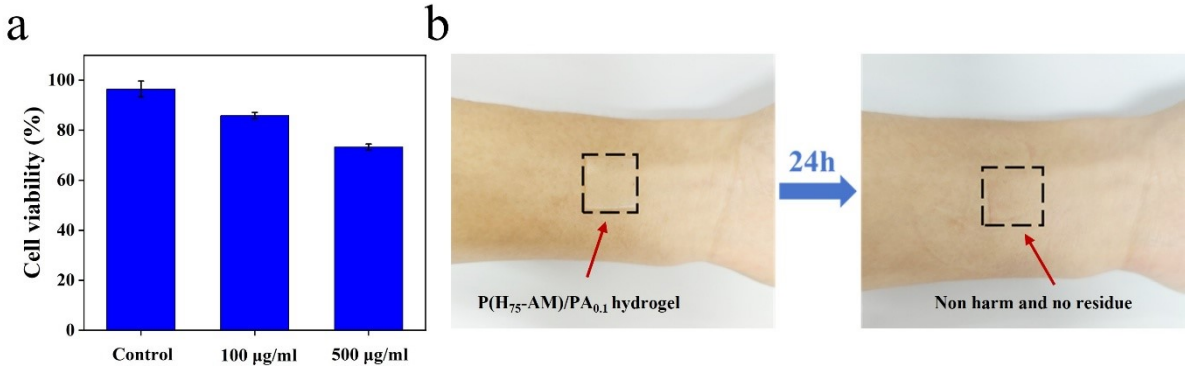

Figure S9. (a) Cell viability of NIH3T3 cells cultured with P(H_{75}-AM)/$PA_{0.1}$ hydrogel extracts for 24 h. (b) A piece of hydrogel adhered on a human arm before and after 24 h.

References

[1]. You, M.; Guo, Y.-X; Yu, H.; Yin, H.-Y; Shi, X.-L; Tang, Z.-Q; Yang, J.; Qin, G.; Shen, J.-L.; Tang, Chen, Q; *Chem. Eng. J.* **2024,** *500*, 157103.

[2]. Di, X.; Hang, C.; Xu, Y.; Ma, Q.-Y; Li, F.-F; Sun, P.-C; Wu, G.-L., *Mater. Chem. Front.,* **2020***, 4, 189-196.*

[3]. Shan, M.; Gong, C; Li, B.-Q; Wu, G.-L; *Polym. Chem.,* **2017***, 8, 2997-3005*

[4]. Wang, Z.; Ma, Z.; Wang, S.; Pi, M.; Wang, X.; Li, M.; Lu, H.; Cui, W.; Ran, R., *Carbohydr. Polym.* **2022,** *298*, 120128.

[5]. Xu, L.; Li, X.; Gao, J.; Yan, M.; Wang, Q., *Mater. Today Commun.* **2024,** *40*, 109542.

[6]. Qiu, H.; Guo, P.; Guan, Y.; Yuan, B.; Li, H.; Wang, H.; Liu, R.; Wang, H.; Zhang, R.; Fu, H.; Cui, W., *Colloids Surf. A Physicochem. Eng. Asp.* **2024,** *686*, 133346.

[7]. Liu, T.; Tang, Z.; Tang, X.-G.; Liang, Z.; Feng, J.; Ye, L.; Tan, Y.; Jiang, Y.-P.; Lan, M.; Zhu, D.; Gong, W., *Colloids Surf. A Physicochem. Eng. Asp.* **2024,** *695*, 134196.

[8]. Xiao, W.; Yang, C.; Wang, W.; Chen, H.; Bai, L.; Yang, H.; Yang, L.; Wei, D., *Mater. Chem. Phys.* **2023,** *310*, 128507.

[9]. Gao, Y.; Wei, C.; Zhao, S.; Gao, W.; Li, Z.; Li, H.; Luo, J.; Song, X., J. Appl. Polym. Sci. **2023,** *140* (3), e53327.

[10]. Li, X.; Zhang, T.; Song, B.; Yang, K.; Hao, X.; Ma, J., Polym. Adv. Technol. **2024,** *35* (1), e6267.

[11]. Zhang, Y.; Wang, S.; Tian, Y.; Chen, L.; Du, Y.; Su, G.; Hu, Y., Polymers. **2023,** *15* (18), 3748.

[12]. Shi, G.; Zhan, T.; Hu, Y.; Guo, Z.; Wang, S., *J. Polym. Res.* **2023,** *30* (2), 61.

[13].Wang, J.; Luo, J.; Jia, Z.; Chen, Y.; Li, C.; Zhong, K.; Xiang, J.; Jia, P., ACS Appl. Polym. Mater. **2024,** *6* (11), 6603-6613.